PROCEEDINGS OF SCIENCE

Searches for direct *CP* violation in quasi-two-body *B* meson decays at LHCb

T. Hadavizadeh[*†], **on behalf of the LHCb collaboration**
University of Oxford
E-mail: tom.hadavizadeh@cern.ch

The decays of *B* mesons with contributions from loop processes give access to physics within and beyond the Standard Model. Measurements of *CP*-violating parameters, branching fractions, and polarisation fractions in processes proceeding via vector mesons help shed light on the relative contributions of the underlying processes. The latest LHCb results involving *B* meson decays to quasi-two-body final states are presented.

European Physical Society Conference on High Energy Physics - EPS-HEP2019 -
10-17 July, 2019
Ghent, Belgium

[*]Speaker.
[†]Corresponding author

PoS(EPS-HEP2019)261

1. Introduction

Direct *CP* asymmetries arise from interference between amplitudes with different strong and weak phases. The relative size of the interference is maximised when the competing amplitudes are of a similar magnitude, and the sines of the weak and strong phase differences are maximal. Therefore, in decays in which the leading amplitude, for example a tree-level process, is suppressed loop-level processes can compete and give rise to measurable interference. The decays of B hadrons with contributions from loop-level amplitudes give access to processes beyond the Standard Model, as heavy particles could contribute within the loops and produce effects that may be observable with current levels of sensitivity.

Quasi-two-body decays provide a powerful laboratory for the study B decays. As well as *CP*-violating effects, quasi-two-body decays that proceed via vector mesons allow the measurement of the polarisation fraction and the S-wave contributions to the same final state. These provide additional handles to help understand the competing contributions to B hadron decays.

Three recent LHCb measurements of quasi-two-body decays are reported in these Proceedings. Each measurement has been performed using pp collision data corresponding to $3\,\text{fb}^{-1}$ of integrated luminosity taken during Run 1 of the LHC. The first performs a measurement of the direct *CP* asymmetry and branching fraction of $B^+ \to J/\psi\,\rho^+$ decays; the second is an amplitude analysis that determines the *CP* asymmetry of $B^0 \to \rho^0 K^{*0}$ decays[1]; and the third is an amplitude analysis of the closely related decays $B^0 \to K^{*0}\overline{K}^{*0}$ and $B_s^0 \to K^{*0}\overline{K}^{*0}$.

2. Measurement of the branching fraction and *CP* asymmetry in $B^+ \to J/\psi\,\rho^+$ decays

The decay $B^+ \to J/\psi\,\rho^+$ proceeds via tree-level and gluonic-penguin processes as illustrated in Fig. 1.

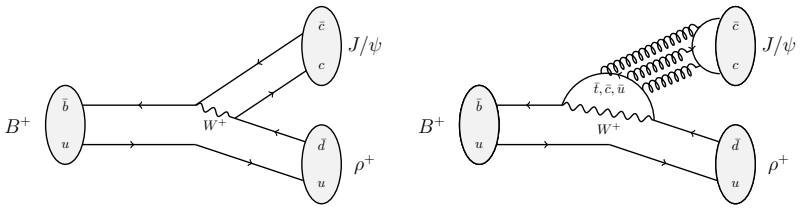

Figure 1: Tree-level and gluonic-penguin processes that contribute to the decays $B^+ \to J/\psi\,\rho^+$.

The direct *CP* asymmetry,

$$\mathscr{A}^{CP} = \frac{\mathscr{B}(B^- \to J/\psi\,\rho^-) - \mathscr{B}(B^+ \to J/\psi\,\rho^+)}{\mathscr{B}(B^- \to J/\psi\,\rho^-) + \mathscr{B}(B^+ \to J/\psi\,\rho^+)}, \tag{2.1}$$

provides an estimate of the imaginary part of the penguin-to-tree amplitude ratio for $b \to c\bar{c}d$ processes. This helps to place constraints on the penguin contributions in the determination of the

[1]Throughout these proceedings ρ^0 is used to refer to the $\rho(770)^0$ resonance and K^{*0} is used to refer to the $K^*(892)^0$ resonance, unless otherwise stated.

CP-violating phase ϕ_s^{cc} from the decay $B_s^0 \to J/\psi\,\phi$. This analysis measures the direct *CP* asymmetry, as well as the branching fraction relative to the abundant $B^+ \to J/\psi\,K^+$ decay [1]. The $B^+ \to J/\psi\,\rho^+$ decays are reconstructed using the $J/\psi \to \mu^-\mu^+$ and $\rho^+ \to \pi^+\pi^0, \pi^0 \to \gamma\gamma$ decay chains. A pre-selection comprised of kinematic, geometrical and vertex-related quantities is performed. In addition, vetoes are applied to target specific peaking backgrounds: invariant mass vetoes remove $B^+ \to J/\psi\,\pi^+$ and $B^+ \to J/\psi\,K^+$ decays that have been combined with an unrelated π^0 meson; and vertex quality requirements remove backgrounds with additional charged tracks. Combinatorial background is reduced by using a multivariate selection. An artificial neutral network is trained using a simulated sample for the signal and a background sample taken from the signal-depleted regions of data, namely the mass sidebands.

A kinematic fit is performed to the data, constraining the J/ψ and π^0 masses to their known values and requiring the B^+ candidate to originate at the primary interaction vertex. A two-dimensional unbinned maximum-likelihood fit is performed to the masses $m(J/\psi\,\pi^+\pi^0)$ and $m(\pi^+\gamma\gamma)$. The result of this fit is shown in Fig. 2.

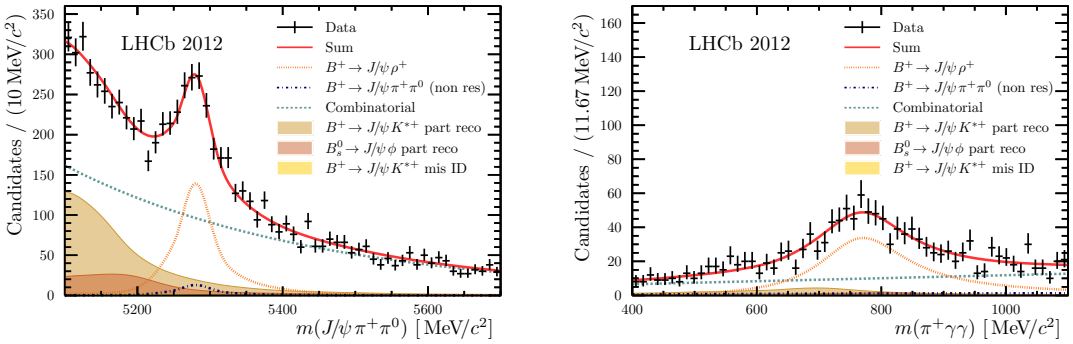

Figure 2: The distribution of $B^+ \to J/\psi\,\rho^+$ candidates in 2012 data in (left) $m(J/\psi\,\pi^+\pi^0)$ and (right) $m(\pi^+\gamma\gamma)$, overlaid with one-dimensional projections of the two-dimensional unbinned maximum-likelihood fit. The distribution of $m(\pi^+\gamma\gamma)$ is restricted to candidates with $m(J/\psi\,\pi^+\pi^0)$ in the range 5250 MeV/c^2 to 5310 MeV/c^2.

The raw asymmetry, $\mathscr{A}^{\rm Raw}$, is determined by fitting the yields of B^+ and B^- candidates in separate categories of the simultaneous fit. The *CP* asymmetry is related to the raw asymmetry as

$$\mathscr{A}^{\rm Raw}(B^+ \to J/\psi\,\rho^+) = \mathscr{A}^{CP}(B^+ \to J/\psi\,\rho^+) + \mathscr{A}^{\rm Prod}(B^+), \tag{2.2}$$

where $\mathscr{A}^{\rm Prod}(B^+)$ is the production asymmetry of the B^+ meson measured to be $(-0.41 \pm 0.49({\rm stat}) \pm 0.11({\rm sys}))\%$ and $(-0.53 \pm 0.31({\rm stat}) \pm 0.10({\rm sys}))\%$ in 2011 and 2012, respectively [2]. The direct *CP* asymmetry and branching fraction are determined to be

$$\mathscr{A}^{CP}(B^+ \to J/\psi\,\rho^+) = -0.045^{+0.056}_{-0.057} \pm 0.008$$

$$\mathscr{B}(B^+ \to J/\psi\,\rho^+) = (3.81^{+0.25}_{-0.24} \pm 0.35) \times 10^{-5},$$

where the first uncertainty is statistical and the second arises as a result of experimental systematic uncertainties. These results are the most precise to date. The main systematic uncertainty on the

branching fraction measurement originates from the π^0 reconstruction efficiency determination. This is calculated using input from the control mode $B^+ \to J/\psi K^{*+}$ and is limited by the precision of the branching fraction $\mathscr{B}(B^+ \to J/\psi K^{*+})$.

3. Study of the $B^0 \to \rho(770)^0 K^*(892)^0$ decay with an amplitude analysis of $B^0 \to (\pi^+\pi^-)(K^+\pi^-)$ decays

Direct *CP* asymmetries are measured in the $B^0 \to (\pi^+\pi^-)(K^+\pi^-)$ final state by determining the differences in partial widths of amplitudes for B^0 and $\bar{B}^0$ decays [3]. The tree-level contribution to the $B^0 \to \rho^0 K^{*0}$ decay is doubly Cabibbo-suppressed, allowing gluonic and electroweak penguins compete, as shown in Fig. 3. In this pseudoscalar to vector-vector decay the final state

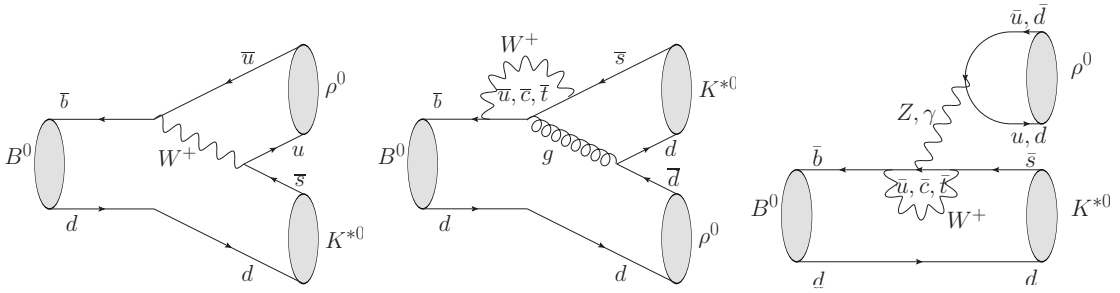

Figure 3: Tree-level, gluonic-penguin and electroweak-penguin decay processes that contribute to the $B^0 \to \rho^0 K^{*0}$ decay.

can be described in three different helicity configurations. The electroweak-penguin amplitudes contribute with different signs for different helicity eigenstates.

The $B^0 \to (\pi^+\pi^-)(K^+\pi^-)$ candidates are selected using a pre-selection, comprised of kinematic, geometric and particle identification requirements, followed by a multivariate selection intended to remove combinatorial background. A BDT algorithm is trained using simulation samples as signal and data in the mass sidebands as background. Vetoes are used to remove specific backgrounds: PID requirements are placed to remove $\Lambda_b^0 \to p\pi^+\pi^-\pi^+$ decays; a veto is placed on the $m(K\pi)$ invariant mass to remove incorrectly paired $B^0 \to D^0\pi^+\pi^-$ decays; and an angular requirement is used to remove three body modes such as $B^0 \to D^-\pi^+$ decays.

A simultaneous unbinned maximum-likelihood fit is performed to the B candidate's invariant mass. The data is split into 8 categories, arising from two trigger selections, two years of data taking and the two B meson charges. Background from $B_s^0 \to (K^+\pi^-)(K^-\pi^+)$ decays is subtracted by injecting simulations with negative weights. The signal component is extracted using the *sPlot* method [4].

An amplitude model is created from different contributions in the $300 < m(\pi^+\pi^-) < 1100\,\text{MeV}/c^2$ and $750 < m(K^+\pi^-) < 1200\,\text{MeV}/c^2$ mass windows. In $\pi^+\pi^-$ mass this includes the ρ^0 and ω vector resonances, along with the scalar $f_0(500)$ and $f_0(1370)$ resonances, described by relativistic spin-0 Breit-Wigner functions, and the $f_0(980)$ resonance, described by a Flatté parameterisation [5, 6]. The $K^+\pi^-$ mass is modelled with a vector K^{*0} and scalar contributions, labelled $(K\pi)_0$. The K^{*0} resonance is described by a spin-1 relativistic Breit-Wigner, and the scalar $(K\pi)_0$ contributions are parameterised by the LASS function [7], modelling the resonant $K_0^*(1430)$ and

non-resonant components. Three helicity amplitudes contribute for each of the vector-vector (VV) combinations ($K^{*0}\rho^0$ and $K^{*0}\,\omega$) and the polarisation fraction is defined to be

$$f_{VV}^{0,\perp,\parallel} = \frac{|A^{0,\perp,\parallel}|^2}{|A^0|^2 + |A^\perp|^2 + |A^\parallel|^2}, \tag{3.1}$$

where the fraction is defined for the longitudinal, perpendicular and parallel amplitudes ($A^{0,\perp,\parallel}$). From these, the *CP* averages, $\tilde{f}_{VV} = (f_{VV} + \overline{f}_{VV})/2$, and asymmetries , $\mathcal{A}_{VV} = (f_{VV} - \overline{f}_{VV})/(f_{VV} + \overline{f}_{VV})$ can be determined, where the quantities f and $\overline{f}$ refer to B^0 and $\bar{B}^0$ decays, respectively. Additionally, the phase differences with respect to the reference channel $B^0 \to \rho^0(K^+\pi^-)$ and triple product asymmetries, as defined in Ref. [8], are measured. One-dimensional projections of the amplitude fit to the B^0 candidates are shown in Fig. 4, along with the contribution from each partial wave (corresponding projections for $\bar{B}^0$ candidates can be found in Ref. [3]).

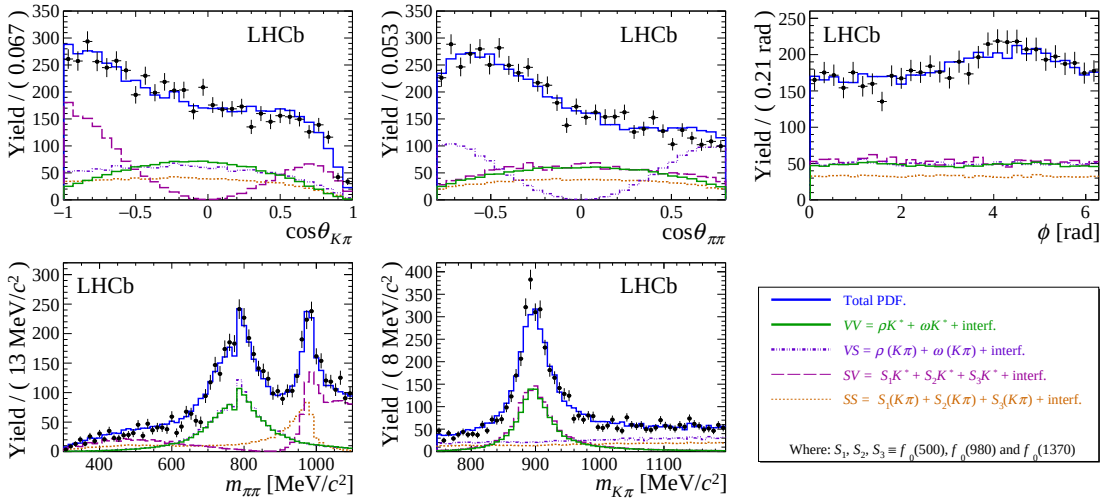

Figure 4: Projections of the amplitude fit to the $B^0 \to (K^+\pi^-)(\pi^+\pi^-)$ final state. The overlaid contributions are grouped by their angular dependencies as described in the legend.

The amplitude analysis finds a small longitudinal polarisation fraction and a significant direct *CP* asymmetry for the $B^0 \to \rho^0 K^{*0}$ component,

$$\tilde{f}^0_{\rho K^*} = 0.164 \pm 0.015 \pm 0.022 \;\text{ and }\; \mathcal{A}^0_{\rho K^*} = -0.62 \pm 0.09 \pm 0.09,$$

where the first uncertainty is statistical and the second systematic. These measurements hint at a relevant contribution from the colour-allowed electroweak-penguin amplitude, and correspond to the first significant observation of *CP* asymmetry in $B^0 \to VV$ decays.

4. Amplitude analysis of the $B^0_{(s)} \to K^{*0}\overline{K}^{*0}$ decays and measurement of the branching fraction of the $B^0 \to K^{*0}\overline{K}^{*0}$ decay

The $B^0 \to K^{*0}\overline{K}^{*0}$ decay is a Flavour Changing Neutral Current process, forbidden at tree level in the standard model. The decay $B^0_s \to K^{*0}\overline{K}^{*0}$ can be used to determine the CKM phase $\phi_s{}^{dd}$, as the sub-leading amplitude is Cabibbo suppressed. However, when making high precision

measurements, input from the $B^0 \to K^{*0}\overline{K}^{*0}$ process can help control the higher-order standard model contributions, assuming U-spin symmetry. Previous measurements suggest the $B^0 \to K^{*0}\overline{K}^{*0}$ decay has a large longitudinal polarisation fraction, whilst the corresponding value for $B^0_s \to K^{*0}\overline{K}^{*0}$ decays is small, in tension with theoretical predictions [9]. Additionally, there is a 2.2 sigma difference between $\mathscr{B}(B^0 \to K^{*0}\overline{K}^{*0})$ as measured by the Belle and BaBar collaborations [10, 11].

This analysis performs an untagged, time-integrated amplitude analysis of $B^0_{(s)} \to (K^-\pi^+)(K^+\pi^-)$ decays, as well as determining the branching fraction $\mathscr{B}(B^0 \to K^{*0}\overline{K}^{*0})$ [12]. Candidates are selected using a pre-selection comprised of kinematic, geometric and particle identification requirements. Combinatorial background is reduced by the use of the gradient-boosted BDT algorithm, trained on simulation samples as signal and data sidebands as background. The invariant mass windows and PID selections suppress many peaking backgrounds, including those with intermediate charm mesons, misidentified tracks or additional final state particles.

A simultaneous extended maximum-likelihood fit is performed to the four-body invariant mass distribution. Contributions from $B^0 \to \rho^0 K^{*0}$ decays are subtracted by injecting simulations with negative weights. The *sPlot* method is used to extract the background-subtracted distributions of the B^0 and B^0_s signal components. Two amplitude analyses are performed on these weighted samples. The amplitude models are built using known resonances that could contribute within the 150 MeV/c^2 $K\pi$ mass windows. This includes a P-wave $K^*_0(892)^0$ resonance, modelled by a spin-1 relativistic Breit-Wigner, and S-wave contributions, namely the $K^*_0(1430)^0$, $K^*_0(700)^0$ and non-resonant $(K\pi)_0$ component. The scalar contributions are modelled using the LASS parameterisation [7]. The one-dimensional projections of the B^0 amplitude fit are shown in Fig. 5, along with the different partial wave contributions. The longitudinal polarisation fractions for the $B^0 \to K^{*0}\overline{K}^{*0}$

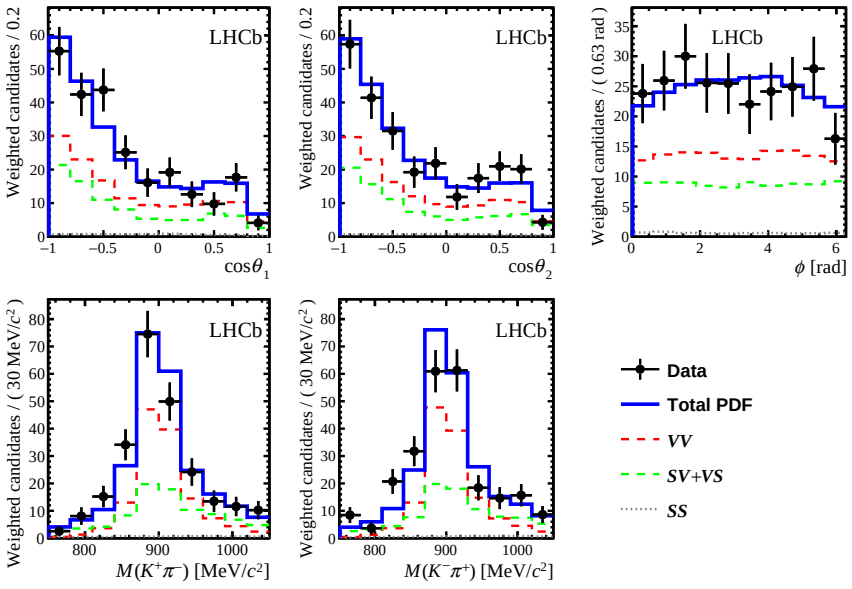

Figure 5: Amplitude fit to the $B^0 \to (K^-\pi^+)(K^+\pi^-)$ final state, along with the contributions from different resonant amplitudes.

$B^0_s \to K^{*0}\overline{K}^{*0}$ decays are measured to be

$$f^0(B^0 \to K^{*0}\overline{K}^{*0}) = 0.724 \pm 0.051 \pm 0.016$$

$$f^0(B^0_s \to K^{*0}\overline{K}^{*0}) = 0.240 \pm 0.031 \pm 0.025,$$

where the first uncertainties are statistical and the second systematic. This confirms the previous measurements. The fractional S-wave contribution is determined from the total of the scalar-scalar, vector-scalar and scalar-vector amplitudes, and found to be $0.408 \pm 0.050 \pm 0.017$ ($0.694 \pm 0.016 \pm 0.010$) for the B^0 (B^0_s) decay. The ratio of branching fractions of the two decays is measured, and used to determine

$$\mathscr{B}(B^0 \to K^{*0}\overline{K}^{*0}) = (8.0 \pm 0.9 \pm 0.4) \times 10^{-7},$$

in agreement with theoretical predictions [9]. This value is smaller than the measurement performed by the BaBar collaboration as a result of the large S-wave contribution. However, using the B^0_s meson averages [13] for $y = \Delta\Gamma/(2\Gamma) = 0.064 \pm 0.005$ and the mixing phase $\phi_s = -0.021 \pm 0.0031$ as defined in Ref. [12], the ratio

$$R_{sd} = \frac{\mathscr{B}(B^0_s \to K^{*0}\overline{K}^{*0})}{\mathscr{B}(B^0 \to K^{*0}\overline{K}^{*0})} \frac{f^0(B^0_s \to K^{*0}\overline{K}^{*0})}{f^0(B^0 \to K^{*0}\overline{K}^{*0})} \frac{1-y^2}{1+y\cos\phi_s} = 3.48 \pm 0.38, \tag{4.1}$$

is found to be inconsistent with the prediction $R_{sd} = 16.4 \pm 5.2$ [14]. This calls into question the predicted hierarchy of polarisation fractions $f^0 \gg f^{\perp,\parallel}$ from the heavy-quark limit.

5. Conclusion

The LHCb experiment has produced measurements for *CP* asymmetries, branching fractions and longitudinal polarisation fractions in quasi-two-body decays with Run 1 data. This includes the most precise *CP* asymmetry and branching fraction of $B^+ \to J/\psi\rho^+$ decays; the observation of *CP* asymmetry in the angular distributions of $B^0 \to \rho^0 K^{*0}$ decays, a first for $B^0 \to VV$ decays; and measurements of both longitudinal polarisation fractions and ratio of branching fractions in $B^0_{(s)} \to K^{*0}\overline{K}^{*0}$ decays. In future, the addition of Run 2 data will further enhance the precision and scope of quasi-two-body measurements at LHCb.

References

[1] LHCb collaboration, *Measurement of the branching fraction and CP asymmetry in $B^+ \to J/\psi\rho^+$ decays*, *Eur. Phys. J.* **C79** (2019) 537 LHCb-PAPER-2018-036 CERN-EP-2018-336, [1812.07041].

[2] LHCb collaboration, *Measurement of the $B^\pm$ production asymmetry and the CP asymmetry in $B^\pm \to J/\psi K^\pm$ decays*, *Phys. Rev.* **D95** (2017) 052005 LHCb-PAPER-2016-054, CERN-EP-2016-325, [1701.05501].

[3] LHCb collaboration, *Study of the $B^0 \to \rho(770)^0 K^*(892)^0$ decay with an amplitude analysis of $B^0 \to (\pi^+\pi^-)(K^+\pi^-)$ decays*, *JHEP* **05** (2019) 026 LHCb-PAPER-2018-042 CERN-EP-2018-316, [1812.07008].

[4] M. Pivk and F. R. Le Diberder, *sPlot: A statistical tool to unfold data distributions*, Nucl. Instrum. Meth. **A555** (2005) 356 [physics/0402083].

[5] S. M. Flatte, *Coupled - Channel Analysis of the $\pi\eta$ and $K\overline{K}$ Systems Near $K\overline{K}$ Threshold*, Phys. Lett. **63B** (1976) 224.

[6] S. M. Flatte, *On the Nature of 0^+ Mesons*, Phys. Lett. **63B** (1976) 228.

[7] D. Aston et al., *A Study of $K^-\pi^+$ Scattering in the Reaction $K^-p \to K^-\pi^+n$ at 11 GeV/c*, Nucl. Phys. **B296** (1988) 493.

[8] A. Datta and D. London, *Triple-product correlations in $B \to V_1V_2$ decays and new physics*, Int. J. Mod. Phys. **A19** (2004) 2505 [hep-ph/0303159].

[9] M. Beneke, J. Rohrer and D. Yang, *Branching fractions, polarisation and asymmetries of $B \to VV$ decays*, Nucl. Phys. **B774** (2007) 64 [hep-ph/0612290].

[10] BABAR collaboration, *Observation of $B^0 \to K^{*0}\bar{K}^{*0}$ and search for $B^0 \to K^{*0}K^{*0}$*, Phys. Rev. Lett. **100** (2008) 081801 [0708.2248].

[11] BELLE collaboration, *Search for $B^0 \to K^{*0}\overline{K}^{*0}$, $B^0 \to K^{*0}K^{*0}$ and $B^0 \to K^+\pi^-K^\mp\pi^\pm$ Decays*, Phys. Rev. **D81** (2010) 071101 [1001.4595].

[12] LHCB collaboration, *Amplitude analysis of the $B^0_{(s)} \to K^{*0}\bar{K}^{*0}$ decays and measurement of the branching fraction of the $B^0 \to K^{*0}\bar{K}^{*0}$ decay*, JHEP **07** (2019) 032 LHCb-PAPER-2019-004 CERN-EP-2019-063, [1905.06662].

[13] HFLAV collaboration, *Averages of b-hadron, c-hadron, and τ-lepton properties as of summer 2016*, Eur. Phys. J. **C77** (2017) 895 [1612.07233].

[14] S. Descotes-Genon, J. Matias and J. Virto, *An analysis of $B_{d,s}$ mixing angles in presence of New Physics and an update of $B^0_s \to K^{*0}\overline{K}^{*0}$*, Phys. Rev. **D85** (2012) 034010 [1111.4882].